

**REAL-TIME CONTROL OF THE SALT FRONT IN A COMPLEX,
TIDALLY AFFECTED RIVER BASIN****EDWIN A. ROEHL**OptiQuest Technologies
Greenville, SC**PAUL A. CONRADS**U.S. Geological Survey
Columbia, SC***ABSTRACT***

The U.S. Geological Survey (USGS) participated in comparing artificial neural networks (ANN's) to deterministic models of transport and water quality phenomena of an estuary in Charleston, SC. The models were developed from real-time data from a gauging network operated by the USGS. The results favored the ANN's accuracy and reduced development time. They could spatially interpolate between gauging stations to predict the location of the freshwater/saltwater interface, called the "salt front". The salt front location depends on the interaction of freshwater flowing downstream from a hydroelectric dam and tidal forcing of saltwater upstream. Government regulations conservatively control dam releases to prevent saltwater migrating into a freshwater reservoir, but sub-optimizes the commercial operation of the dam. This paper describes an alternative control approach using an ANN model of the "gain" between the freshwater releases and the specific conductivity, used to estimate salinity, near the reservoir. A scheme for implementing the model in a real-time control system is also described.

INTRODUCTION

A problem of great social and environmental importance is determining how to best use natural resources while preserving the quality of surrounding natural systems, such as surface water, groundwater, and atmospheric systems. Environmental regulatory agencies attempt to control exploitation using scientific means such as deterministic (physics-based) models that predict how a natural system will behave under scenarios of interest. In practice it is commonly found that the statistical accuracy of the models is poor because natural systems can be too complex for state-of-the-art deterministic modeling methods. This results in important decisions being made in the absence of unambiguous scientific findings.

The U.S. Geological Survey (USGS) participated in comparing artificial neural network (ANN's) models to deterministic finite-difference models of the Cooper River, a complex estuarine system shown in Fig. 1 (Conrads and Roehl, 1999). Both models were developed from three years of real-time measurements of water level (WL), dissolved-oxygen concentration, water temperature, and specific conductivity (SC, used to compute salinity) that had been collected by a network of gauging stations. The models predicted the river's hydrodynamic, mass transport, and water-quality behaviors. The ANN's were found to be

significantly more accurate and quickly developed. Their compactness and fast execution allowed their use in a prototype control system that was used to investigate regulating wastewater discharges according to the river's assimilative capacity (Roehl and Conrads, 1999).

Subsequently, ANN models were configured to spatially interpolate between gauging stations to predict WL and SC at arbitrary locations within the gauging network (Fig. 2). Of particular interest was predicting the "salt front" location, which is normally in the vicinity of station 02172053 (hereafter "s" replaces the station prefix 021720). This result pointed to a solution for protecting a valuable freshwater reservoir from saltwater migration. A canal located 10 km above s50 connects the west branch of the Cooper River to the reservoir.

The location of the salt front depends on tidal conditions and the volume of freshwater flowing downstream from a hydroelectric dam on Lake Moultrie. The WL's power spectrum revealed a strong 28-day lunar cycle. Low freshwater flows coinciding with high tidal levels allows seawater to migrate towards the canal. Figure 3 shows that the SC at s50 peaks a few tidal cycles after peaking at s53 due to upstream migration of the salt front.

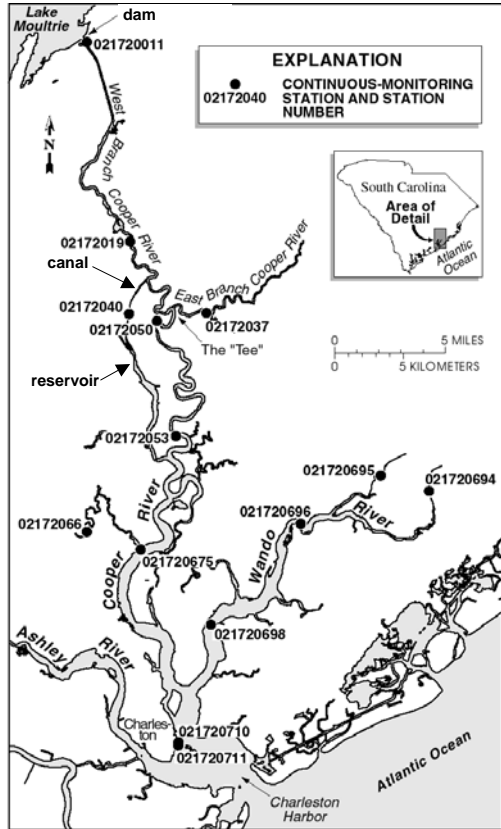


Figure 1. The Cooper and Wando River, SC.

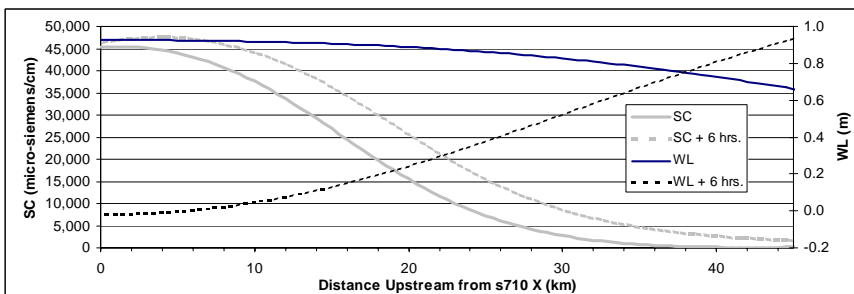


Figure 2. ANN model's spatially interpolated SC and WL for one tidal cycle six hours apart.

Government regulations require minimum total weekly flows from the dam meet water supply demands, however, the timing of the releases is at the discretion of hydroelectric dam operators. The power utility has implemented a number of “action alert thresholds”, which when exceeded, require that flows be increased above minimum levels. The SC threshold at s50, which is nearest to the canal, is 1,500 micro-siemens per centimeter ($\mu\text{s}/\text{cm}$), however, it rarely comes into play because thresholds for stations further downstream are exceeded some 20 to 30 times per year. The optimum user of power generation from the dam is to meet peak power demands. When water is released to control the salt front it significantly undermines the commercial operation of the dam.

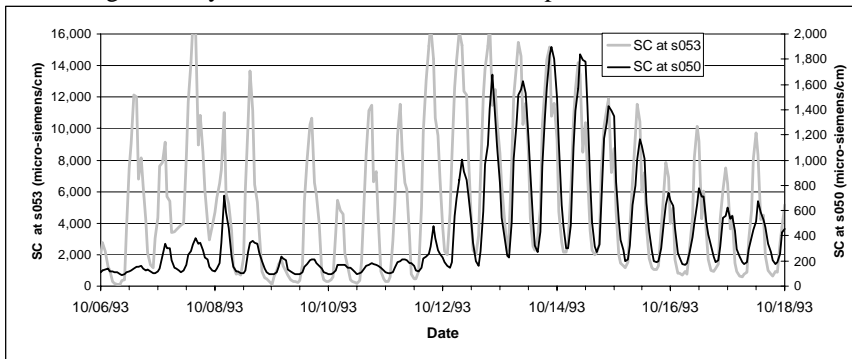


Figure 3. Detail of actual SC at s53 and s50 (30 and 45 km upstream of s710 respectively).

Below is an alternative to the above regulatory control approach. It fully utilizes the data from the gauging stations to optimize the control of the freshwater releases, bringing significant benefit to the utility. The scheme uses ANN-based models to predict and control the location of the salt front in real-time.

DATA PREPARATION

The data used for analysis and modeling was comprised of hourly measurements of the SC and WL at s011 at the base of the dam, at s50 10 km below the entrance to the canal, and at s710 at the mouth of the Cooper River. s50 and s011 are approximately 45 and 75 km upriver from s710, respectively. These data were reduced to remove missing or unreliable measurements to arrive at 16,384 (2^{14}) hourly time stamps suitable for filtering by methods using the Fast Fourier Transform (Press et al, 1993). The 30 km separating s011 and s50 made it apparent that the response time between control actions taken at the dam and subsequent changes in the salt front could be several days. Therefore, variables were filtered to remove frequencies at or greater than the 24-hour diurnal cycle. The data were bifurcated into a 20/80 ratio of training and test data for synthesizing feed-forward ANN models.

MODELING THE GAIN

The “gain” describes the relationship between a controlled variable (CV) and a variable that is manipulated (MV) to control the CV. For the salt front

problem, the CV is the SC at s50 and the MV is the WL at s011, which is a surrogate for volumetric releases from the dam. Figure 4 shows that the WL at s011 exhibits the same 12.4-hour tidal cycle, delayed by 10 hours, as the WL at the river's mouth 75 km downstream. Differences in the filtered signals suggested that the WL is additionally influenced by freshwater releases. These observations indicated that the WL signal at the dam should be separated into two components, one corresponding to the tidal cycle and the other to the dam releases, the latter to be used to determine the gain.

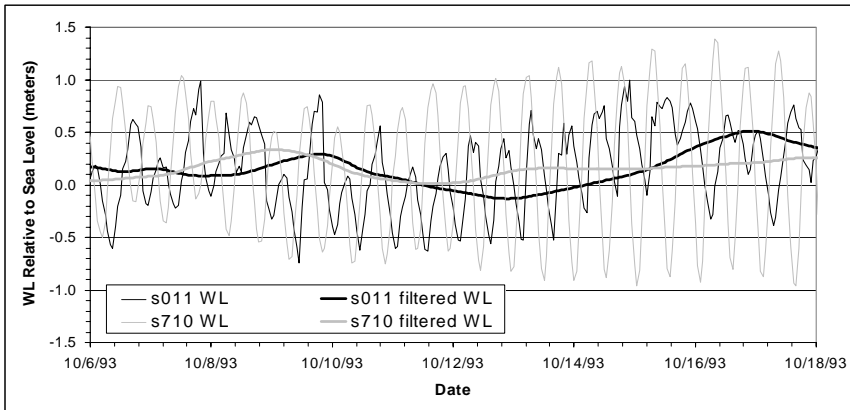


Figure 4. Detail of actual and filtered WL at s011 and s710.

Separating the signal involves the construction of a function that correlates the WL at the dam to the WL at the river's mouth. For the function's input, the WL at s710 was selected over WL's from upriver stations because it is the least likely to be influenced by the dam releases. Linear correlation (Press et al, 1993) can relate the time series of one variable to that of another. It can also relate a current measurement of a variable to past measurements of the same variable. Successive shifting of one time series relative to another (or to itself) by a delay τ_d , while computing the correlation for each shift, provides information indicating when the correlation reaches maximum, minimum, and zero values. The first delay at which the correlation equals (or nears) zero is the delay τ_z at which the times series are "decorrelated".

The bivariate function that was used to correlate the WL's at s011 and s710 is derived from an approach applied to univariate chaotic time series (Abarbanel, 1996). Equation (1) suggests that at time t , a predicted value x_p for variable x can be computed from previous, actual measurements x_a by a function F . The "local dimension" d_L specifies the number of measurements required to optimally predict x_p . Note that $x_p(t) = x_a(t)$ at $\tau_d = 0$, and the predictive accuracy of F declines towards zero as τ_d approaches τ_z .

$$x_p(t) = F [x_a(t-\tau_d), x_a(t-(\tau_d+\tau_z)), \dots, x_a(t-(\tau_d+k\tau_z)), \dots, x_a(t-(\tau_d+(d_L-1)\tau_z))], 0 < \tau_d < \tau_z \quad (1)$$

The bivariate form of Eq. 1 is given by Eq. (2), which relates y and x , the WL's at s011 and s710 respectively. Predictions y_p are computed from actual measurements x_a by the function F_1 . Comparing Eqs. (1) and (2), τ_d is replaced

by the delay τ'_d at which y is maximally correlated to x , while d_L and τ_z remain characteristics of only x . The residual y_r given by Eq. (3) is the difference between the actual and predicted measurements, y_a and y_p .

$$y_p(t) = F_1[x_a(t-\tau'_d), x_a(t-(\tau'_d+\tau_z)), \dots, x_a(t-(\tau'_d+k\tau_z)), \dots, x_a(t-(\tau'_d+(d_L-1)\tau_z))]; \tau'_d > 0 \quad (2)$$

$$y_r(t) = y_a(t) - y_p(t) \quad (3)$$

Within the accuracy limits of F_1 and y_a , y_r contains information about the behavior of y that is unrelated to the tidal effects seen at the river's mouth. This information includes but is not limited to freshwater releases from the dam, therefore, y_r can be used to estimate the gain that relates changes in the WL at the dam to the SC at s50, denoted by y and y_2 respectively. Equation (4) was used to compute predictions y_{2p} . It was expected that the gain would also depend on tidal conditions, so that F_2 includes information from both y_r and y_p . Note that F_2 uses different delays and local dimensions in relating y_r and y_p to y_2 .

$$y_{2p}(t) = F_2\{ [y_p(t-\tau'_{pd}), y_p(t-(\tau'_{pd}+\tau_{pz})), \dots, y_p(t-(\tau'_{pd}+m\tau_{pz}))], \dots, y_p(t-(\tau'_{pd}+(d_{pL}-1)\tau_{pz}))], \quad (4)$$

$$[y_r(t-\tau'_{rd}), y_r(t-(\tau'_{rd}+\tau_{rz})), \dots, y_r(t-(\tau'_{rd}+n\tau_{rz}))], \dots, y_r(t-(\tau'_{rd}+(d_{rL}-1)\tau_{rz}))]; \tau'_{pd}, \tau'_{rd} > 0$$

The application of Eq. 2 was as follows. τ'_d and τ_z were determined to be 10 and 30 hours respectively. F_1 was synthesized from time series of x_a and y_a by a feed-forward ANN. The ANN was trained using back-propagation and conjugate gradient methods. A $d_L \approx 8$ was determined experimentally by adding and removing inputs at delays spaced by τ_z and tracking the predictive performance of F_1 . It was also determined that up to two inputs with delays less than $d_L \tau_z$ could be omitted without significantly degrading F_1 . A plot of the predictions made by F_1 and the actual WL are shown in Fig. (5).

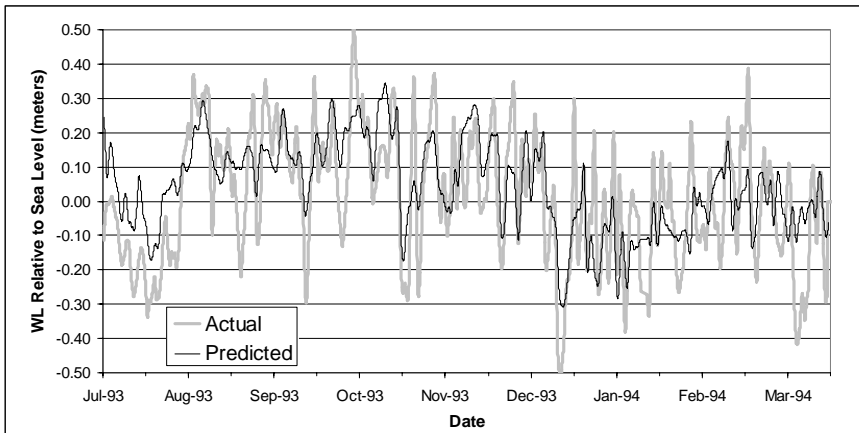


Figure 5: Detail of actual and predicted filtered WL at s011.

The application of Eq. 4 was as follows. The peak correlation τ'_{pd} between y_p and y_2 occurred at 0 hours, indicating that the SC at s50 and the WL at s011 move in phase. A high pass filter with a lower limit of 28 days was applied to y_p to remove apparent annual periodicity, whereupon τ_{pz} was calculated to be 30 hours (the same as τ_z). The delay τ'_{rd} of the peak correlation between y_r and y_{2a}

was 47 hours, indicating a transport delay of about two days between dam releases and a subsequent effect on the SC. τ_{rz} was computed to be 69 hours. A second ANN was developed to synthesize F_2 . The rationale for using a single ANN, which combined inputs for both y_r and y_p , was that they were decorrelated by means of their derivation (also verified by correlation analysis). Local dimensions $d_{rL} \approx 6$ and $d_{pL} \approx 8$ were estimated as described above for d_L . A plot of the prediction made by F_2 and the actual SC is shown in Fig. 6.

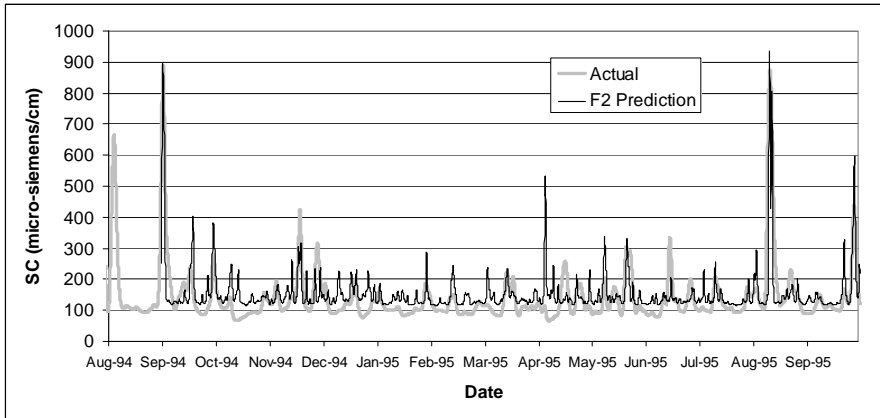


Figure 6. Detail of actual and predicted filtered SC at s50.

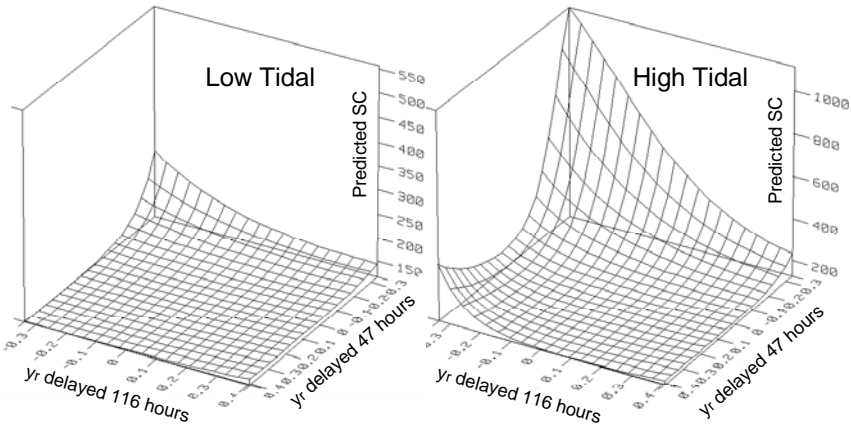


Figure 7. Predicted SC at s50 on dam releases during low and high tidal levels.

The gain of F_2 is better understood by viewing the function's response surface under different tidal conditions. Figure 7 shows that the gain's sensitivity to the first two residual inputs $y_r(t-\tau'_{rd})$ and $y_r(t-(\tau'_{rd}+\tau_{rz}))$, indicated by the difference between the surface's high and low points, varies from 100 to 1,000 $\mu\text{s}/\text{cm}$ at low and high tidal levels. Note that F_2 was developed from hourly data which filtering effectively averaged over two tidal cycles. Thus, the 1,000 $\mu\text{s}/\text{cm}$ gain corresponds to an unfiltered range of about 1,900 $\mu\text{s}/\text{cm}$ (see

Fig. 3). Therefore, the 1,500 $\mu\text{s/cm}$ threshold at s50 is well within the interpolative range of F_2 .

PREDICTION AND CONTROL

The primary intent of this study was to determine the potential of using an ANN-based real-time control scheme to modulate dam releases to control the salt front. The development of a usable model F_2 of the gain between dam releases and their effect on the salt front was a necessary first step. The remaining steps for completing the control scheme are outlined below.

Effective control requires predicting ahead of time if salt front migration will pose a problem to allow time for corrective action. A model that predicts SC at s50 47 hours into the future (equal to τ'_{rd}) is needed. F_2 is unsuitable because it includes $\tau'_{pd}=0$; however, another model F_3 , identical to F_2 but with $\tau'_{pd} = \tau'_{rd}$, was synthesized to show feasibility. The predictions of F_3 , shown in Fig. 8, were poorer than those of F_2 , but it was able to predict some of the events corresponding to the largest values of y_{2a} . F_3 could be easily improved by using additional gauging station variables.

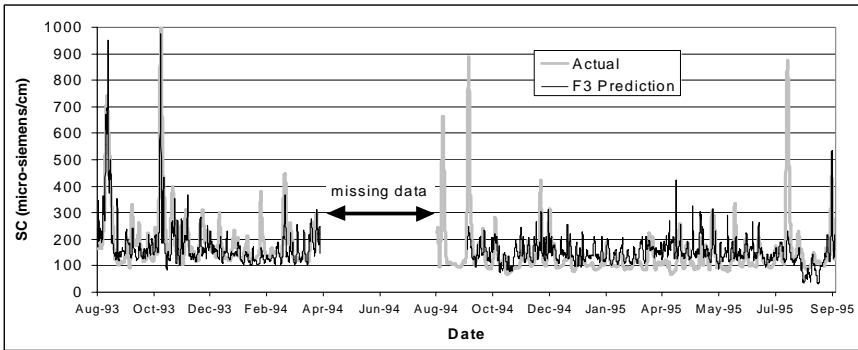


Figure 8. Actual and predicted filtered SC at s50.

Figure 9 shows an idealized model-based control scheme for controlling the salt front, which has been borrowed from the field of industrial process control. Three types of variables are indicated. The variable to be controlled (CV) is the output of the model. Variables that are manipulated (MV) to take corrective action are inputs to the model. Additional inputs are the disturbance variables (DV) that describe the state of the process but cannot be manipulated. Finding values for the MV's so that an undesirable outcome can be avoided requires an optimization program. As DV's change with time, the optimization program searches for MV values that avoid letting the model predict an undesirable outcome. The optimization program adheres to "constraints" that limit the allowable values of the MV's. If

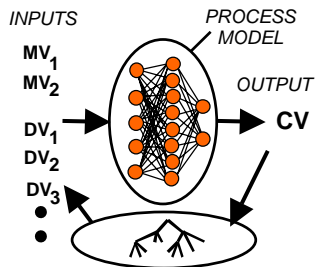


Figure 9. Idealized controller uses an ANN-based process model with an optimization

it fails to obtain an acceptable outcome within a specified number of iterations, the program returns values that minimize the deviation from a desirable outcome.

For this application, F_2 is the process model, the CV is y_{2p} , the MV is $y_r(t-\tau'_{rd})$, and the DV's are the remaining values specified by Eq. (4). A minor problem is that because $\tau'_{pd}=0$ and $t=+47$ hours into the future, the DV $y_p(t-\tau'_{pd})$ is unknown. However, a good estimate can be synthesized from Eq. 2 using $\tau'_{d}=47$ hours. As new values for the DV's are input with each time step, the optimization program's is to compute values for the MV that causes the model to predict a CV that is at or below the 1,500 $\mu\text{s/cm}$ threshold at s50.

DISCUSSION AND CONCLUSIONS

A source of error in the ANN-based functions is the inherent quality of the field data used for their derivation. This is somewhat mitigated by the large number of measurements over widely ranging conditions used for this study. A second problem may lie in the approach used to synthesize F_1 and F_2 . ANN's are an excellent method for regressing data, however, they are subject to a strong tendency for overfitting when correlated inputs are used. Separating inputs by integer multiples of τ_z insures that they are at least linearly decorrelated, but may also sub-optimize F_1 and F_2 which use non-linear ANN's.

Possible improvements could come from several directions. One would be to use actual flow measurements from the dam instead of the surrogate WL at s011. Including additional information from the plethora of variables available from throughout the gauging network might lead to dramatic improvements in prediction accuracy. The investigation of alternative non-linear calculation methods for τ_z , such as average mutual information (Abarbanel, 1996) or single-input-single-output ANN's, may also be beneficial.

Leaving ample room for refinement, the above approach has revealed relationships between measured variables that match a qualitative understanding of this very complex estuarial system. The straightforward mechanics of constructing the various components of the application point to a reliable solution to controlling the location of the salt front. Earlier work in applying these methods to water quality, which is also affected by saltwater migration, suggest combining these problems because of their commonality in serving the public interest.

REFERENCES

- Abarbanel, H.D.I. (1996), Analysis of Observed Chaotic Data, Springer-Verlag New York, Inc., New York, pp. 13-67.
- Conrads, P.A., and Roehl, E.A. (1999), "Comparing Physics-Based and Neural Network Models for Predicting Salinity, Water Temperature, and Dissolved-Oxygen Concentration in a Complex Tidally Affected River Basin," South Carolina Environmental Conference, Myrtle Beach, March 15-16.
- Press, William H., Teukolsky, S.A., Vetterling, W.T., and Flannery, B.P. (1993), Numerical Recipes in C: The Art of Scientific Computing, Cambridge University Press.
- Roehl, E.A., and Conrads, P.A. (1999), "Real-Time Control for Matching Wastewater Discharges to the Assimilative Capacity of a Complex, Tidally Affected River Basin," South Carolina Environmental Conference, Myrtle Beach, March 15-16.